# Quantum interferometry in multimode systems

J. Chwedeńczuk
*Faculty of Physics, University of Warsaw, ulica Pasteura 5, PL-02-093 Warszawa, Poland*
(Received 9 June 2017; published 12 September 2017)

We consider the situation when the signal propagating through each arm of an interferometer has a complicated multimode structure. We demonstrate that the shot-noise level for such a setup is the same as for the common two-mode case for as long as the interferometric transformation treats each arm as a whole and does not penetrate its inner structure. We find the relation between the particle entanglement and the possibility to surpass the shot-noise limit of the phase estimation. Our results are general—they apply to pure and mixed states of identical and distinguishable particles (or combinations of both) for a fixed and fluctuating number of particles. An important result is that the method for detecting the entanglement often used in a two-mode system—based on the measurement of the visibility of fringes and the population imbalance fluctuations—can give misleading results when applied to the multimode case. Our main result is that the additional modes do not boost the sensitivity for as long as they are not interacting. Therefore, the improvement above the shot-noise level established for the two-mode systems can safely be treated as an entanglement criterion also in the complex multimode case.

DOI: 10.1103/PhysRevA.96.032320

## I. INTRODUCTION

Interferometers, the most precise metrological instruments constructed by humans, have played a major role in many breakthrough experiments. In the famous Michelson-Morely failed attempt to detect the ether, the device, now called the "Michelson interferometer," was used [1]. The negative result of this experiment was relevant for the subsequent formulation of the special theory of relativity. Almost 130 yr later, the Laser Interferometer Gravitational-Wave Observatory (LIGO) team used a similar Michelson setup to detect the gravitational wave coming from a collision of two black holes, which took place over $10^9$ yr ago [2]. At the moment of the detection, the sensitivity of the LIGO instruments was high enough to observe the displacement $\Delta L$ of the test masses $\sim 10^{-22}$ times smaller than the length $L$ of the interferometric arms. With $L \simeq 4$ km, this gives a truly impressive $\Delta L \simeq 10^{-19}$ m, which is $\sim 10^3$ times smaller than the radius of a proton.

Matter-wave interferometers at this moment can measure the gravitational acceleration $g$ with the sensitivity of $\Delta g \simeq 10$ nm/s [3–9]. Once miniaturized, such a device could serve as an ultraprecise geological instrument. An atomic interferometer can precisely measure the close to the surface Casimir-Polder forces [10–14]. Once these interactions are well known, the gravitational constant $G$ could be measured by putting an atomic interferometer close to a massive object. Such an experiment could also yield some information about the possible deviations from the Newton $1/r^2$ scaling of the gravitational force at short distances [15]. The gravity-field curvature has recently been observed [16] using an atomic interferometer. Interference of the matter waves also is used in the ultraprecise measurements of the fine-structure constant $\alpha$, which is of fundamental importance [17–21].

At the current stage, these devices operate at best at the shot-noise level, i.e., the sensitivity of the estimation of the parameter $\theta$ does not break the shot-noise limit (SNL) $\Delta\theta \propto \frac{1}{\sqrt{N}}$. Here $N$ is the number of probes—for instance, atoms or photons—which carry the information about the interferometric phase. However, theoretical results and multiple proof-of-principle experiments show that the entanglement between these probes is a resource for the sub-shot-noise (SSN) sensitivity [22,23]. Those experiments follow different routes to create nonclassical states of light or matter. For instance, the LIGO interferometer already displayed the SSN sensitivity when one of its input ports was fed with a squeezed state of light [24]. For interferometers operating on matter waves, the nonclassicality is associated with the entanglement between the particles. This effect often manifests through the spin squeezing of the sample [25–30]. It is a phenomenon—quantified by the spin-squeezing parameter [31,32]—associated with the two-mode algebra. The use of this algebra is quite natural when discussing the interferometric problems—the two arms are identified with the two modes. Most of the interferometric arguments, such as that relating the entanglement to the SSN sensitivity, also are invoked within this two-mode description. However, in principle, the signal propagating through each arm can have a rich multimode structure. This might be a result of thermal excitations as witnessed in Ref. [25] or the inherently multimode nature of the process generating the entangled sample as in Refs. [33–37].

Here we generalize the central theorem of quantum metrology—that relating the SSN sensitivity to the entanglement—to the case when each arm of the interferometer has a complicated multimode structure [38]. The main result of this paper is that the addition of noninteracting modes inside each arm of the interferometer does not have a positive impact on the sensitivity as compared to the standard two-mode case. We show that the particle entanglement remains the key resource for beating the SNL. Our proof is of complete generality—it does not make any assumption about the state and works for identical and distinguishable particles or a combination of both. Also, it applies to systems with a fixed or fluctuating number of particles. We derive the sensitivity of the phase estimation from the measurement of the population imbalance between the two arms. Finally, we show how the method of detecting the particle entanglement, which works for the two-mode systems, can incorrectly indicate the presence of nonclassical correlations in the multimode configurations.

 

This paper is organized as follows. In Sec. II we derive the relation between the entanglement and the SSN sensitivity for identical (Sec. II A) and distinguishable particles (Sec. II B). Other configurations are discussed in Sec. II C. In Sec. III we calculate the phase sensitivity for the estimation based on the knowledge of the average population imbalance between the two arms. In Sec. IV we show that the entanglement witness, often used for two-mode systems, can give false results in the multimode setups. A summary is contained in Sec. V.

## II. ENTANGLEMENT AND SSN SENSITIVITY IN MULTIMODE SYSTEMS

### A. Bosons

#### 1. *Multimode interferometric transformations*

Let $a$ and $b$ denote the two arms of an interferometer. Here, for illustration, we will assume that these arms are spatially separated, however it could be the momentum or other degree of freedom, such as the fine structure, that distinguishes $a$ from $b$. In the standard two-mode case, with each arm, a single operator $\hat{a}$ and $\hat{b}$ is associated. The interferometric transformations are generated by the angular momentum operators,

$$\hat{J}_x = \frac{1}{2}(\hat{a}^\dagger \hat{b} + \hat{b}^\dagger \hat{a}), \tag{1a}$$

$$\hat{J}_y = \frac{1}{2i}(\hat{a}^\dagger \hat{b} - \hat{b}^\dagger \hat{a}), \tag{1b}$$

$$\hat{J}_z = \frac{1}{2}(\hat{a}^\dagger \hat{a} - \hat{b}^\dagger \hat{b}). \tag{1c}$$

To account for the multimode structure of each arm, we introduce the bosonic field operator $\hat{\Psi}(\mathbf{r})$ which consists of two parts, i.e.,

$$\hat{\Psi}(\mathbf{r}) = \hat{\Psi}_a(\mathbf{r}) + \hat{\Psi}_b(\mathbf{r}). \tag{2}$$

Our aim is to construct the interferometric transformation which will act on the multimode arms $a$ and $b$, rather than on two modes only. It is clear that such operations can be constructed in many different ways and that the interferometer's performance depends on the structure of the regions as well as on our choice of transformation. To limit the number of possibilities, we will first assume that the mode structure of $a$ and $b$ is the same, and it is only the spatial separation that makes the distinction between them, see Fig. 1. Therefore, each operator can be expanded into its corresponding basis,

$$\hat{\Psi}_a(\mathbf{r}) = \sum_n \psi_a^{(n)}(\mathbf{r})\hat{a}_n, \tag{3a}$$

$$\hat{\Psi}_b(\mathbf{r}) = \sum_n \psi_b^{(n)}(\mathbf{r})\hat{b}_n, \tag{3b}$$

and the spatial wave functions are shifted by $\mathbf{d}$, i.e.,

$$\psi_b^{(n)}(\mathbf{r}+\mathbf{d}) = \psi_a^{(n)}(\mathbf{r}). \tag{4}$$

Also, we assume $|\mathbf{d}|$ to be much larger than the characteristic widths of the wave packets, giving

$$\psi_a^{(n)}(\mathbf{r})\psi_b^{(m)}(\mathbf{r}) = 0 \quad \forall\, n,m. \tag{5}$$

Once the spatial structure of the system is determined, we pick the interferometric transformations. To establish the analogy with the two-mode case, we consider two types of transformations—the mode mixing and the phase imprint. An extension of (1) is

$$\hat{J}_x = \frac{1}{2}\int d\mathbf{r}[\hat{\Psi}_a^\dagger(\mathbf{r})\hat{\Psi}_b(\mathbf{r}+\mathbf{d}) + \hat{\Psi}_b^\dagger(\mathbf{r}+\mathbf{d})\hat{\Psi}_a(\mathbf{r})], \tag{6a}$$

$$\hat{J}_y = \frac{1}{2i}\int d\mathbf{r}[\hat{\Psi}_a^\dagger(\mathbf{r})\hat{\Psi}_b(\mathbf{r}+\mathbf{d}) - \hat{\Psi}_b^\dagger(\mathbf{r}+\mathbf{d})\hat{\Psi}_a(\mathbf{r})], \tag{6b}$$

$$\hat{J}_z = \frac{1}{2}\int d\mathbf{r}[\hat{\Psi}_a^\dagger(\mathbf{r})\hat{\Psi}_a(\mathbf{r}) - \hat{\Psi}_b^\dagger(\mathbf{r})\hat{\Psi}_b(\mathbf{r})]. \tag{6c}$$

The shift represents the symmetry of the system shown in Fig. 1, however the particular form of the $a/b$ coupling is not relevant for as long as the particle is copied exactly from one region to the other.

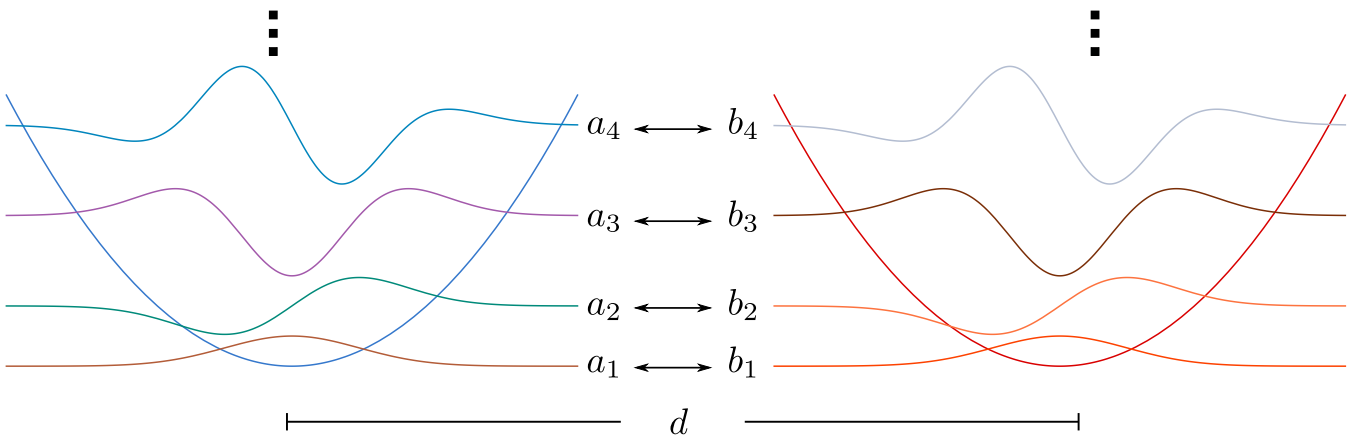


FIG. 1. The two-arm multimode interferometer, illustrated here with the eigenmodes of the harmonic oscillator. Each arm (here a harmonic well) has the same ladder of states, just shifted by $d$. The interferometric transformation can either imprint the relative phase between the arms or move the particles from one arm to the other.

The integrals (6) can be calculated using relations (4) and (5), and the outcome is

$$\hat{J}_x = \frac{1}{2}\sum_n (\hat{a}_n^\dagger \hat{b}_n + \hat{b}_n^\dagger \hat{a}_n) \equiv \sum_n \hat{J}_x^{(n)}, \tag{7a}$$

$$\hat{J}_y = \frac{1}{2i}\sum_n (\hat{a}_n^\dagger \hat{b}_n - \hat{b}_n^\dagger \hat{a}_n) \equiv \sum_n \hat{J}_y^{(n)}, \tag{7b}$$

$$\hat{J}_z = \frac{1}{2}\sum_n (\hat{a}_n^\dagger \hat{a}_n - \hat{b}_n^\dagger \hat{b}_n) \equiv \sum_n \hat{J}_z^{(n)}. \tag{7c}$$

Therefore, the mode mixing operators act on each pair of modes separately. This is a result of 1°, the assumption about the symmetry between the regions, and 2°, the particular form of the coupling in Eqs. (6). Although 1° can be regarded as unnatural or highly idealistic, such symmetry is encountered, for instance, in twin-beam configurations formed by the scattering of atoms from a Bose-Einstein condensate [39]. On the other hand, 2° seems a natural choice: The interferometer should simply "copy" a particle from one arm to another. This second condition can be expressed in other words: The interferometric transformation does not use any knowledge about the internal structure of the arms. It treats each arm as a whole and does not penetrate the inner structure.

The multimode interferometric transformations, which are single-particle operations (i.e., do not entangle the resources), usually are considered in a form

$$\hat{U}(\theta) = e^{-i\theta \hat{J}_n}. \tag{8}$$

Here $\hat{J}_n = \vec{n}\cdot\hat{\vec{J}}$ is a scalar product of a unit vector $\vec{n}$ and a vector of the angular momentum operators [40]. We now will demonstrate that, in analogy to the two-mode case, the particle entanglement is a necessary resource for beating the shot-noise limit of the phase estimation also in the multimode case.

### 2. *Role of the particle entanglement*

Let us begin with a two-mode separable (i.e., nonentangled) pure state of $N$ bosons. It is the spin-coherent state,

$$|z,\varphi;N\rangle = \frac{1}{\sqrt{N!}}(\sqrt{z}e^{i\varphi}\hat{a}^\dagger + \sqrt{1-z}\hat{b}^\dagger)^N|0\rangle. \tag{9}$$

Here, $z \in [0,1]$ is the population imbalance between the two modes, whereas $\varphi \in [0,2\pi]$ is the relative phase. This state is a basic building block of the density matrix of $N$ nonentangled bosons, which reads

$$\hat{\varrho}_{\rm sep} = \int_0^1 dz \int_0^{2\pi} d\varphi\, \mathcal{P}(z,\varphi)|z,\varphi;N\rangle\langle z,\varphi;N|, \tag{10}$$

where $\mathcal{P}$ is a probability distribution of the variables $(z,\varphi)$. The expression (10) is the fixed-$N$ analog of the classical state of the electromagnetic field, according to the Glauber-Sudarshan criterion [41–44]. The expressions (9) and (10) can easily be generalized to the multimode setup. Namely, the former transforms to

$$|z,\varphi;N\rangle \to |\vec{\alpha},\vec{\beta};N\rangle = \frac{1}{\sqrt{N!}}(\vec{\alpha}\hat{\vec{a}}^\dagger + \vec{\beta}\hat{\vec{b}}^\dagger)^N|0\rangle. \tag{11}$$

The vectors of complex amplitudes $\vec{\alpha}$ and $\vec{\beta}$ are normalized, i.e, $|\vec{\alpha}|^2 + |\vec{\beta}|^2 = 1$, whereas $\hat{\vec{a}}$ and $\hat{\vec{b}}$ are vectors of mode operators introduced in Eq. (3). Similarly, the density matrix of unentangled bosons now reads [45]

$$\hat{\varrho}_{\rm sep} = \iint d\vec{\alpha}\, d\vec{\beta}\, \mathcal{P}(\vec{\alpha},\vec{\beta})|\vec{\alpha},\vec{\beta};N\rangle\langle\vec{\alpha},\vec{\beta};N|. \tag{12}$$

We will show that, for the separable states (12) and the interferometric transformations (8), the phase estimation sensitivity is bounded by the shot noise.

The sensitivity of the phase estimation is limited by the Cramer-Rao lower bound [46],

$$\Delta\theta \geqslant \frac{1}{\sqrt{m}}\frac{1}{\sqrt{F_q}}. \tag{13}$$

Here, $m$ is the number of the independent repetitions of the estimation experiment. The $F_q$ is called the quantum Fisher information (QFI), and it quantifies the amount of information about $\theta$, which can be extracted from $m$ measurements using any estimation strategy [47]. For pure states, the QFI is simple to calculate

$$F_q = 4\left(\langle \hat{J}_n^2\rangle - \langle \hat{J}_n\rangle^2\right) \equiv 4\langle(\Delta\hat{J}_n)^2\rangle, \tag{14}$$

where the expectation value is calculated with the state undergoing the interferometric transformation. For mixed states, the QFI is much more complex,

$$F_q = 2\sum_{i,j}\frac{(p_i - p_j)^2}{p_i + p_j}|\langle i|\hat{J}_n|j\rangle|^2, \tag{15}$$

where $|i/j\rangle$ are the eigenvectors and $p_{i/j}$ are the corresponding eigenvalues of the density matrix. Therefore, to obtain $F_q$, one would need to diagonalize $\hat{\varrho}_{\rm sep}$ from Eq. (12), which is numerically feasible but analytically very hard since different $|\vec{\alpha},\vec{\beta};N\rangle$'s are not orthogonal, just as nonorthogonal are the coherent states of light. However, a useful feature of the QFI—its convexity—allows to lower bound the sensitivity for mixed states. Namely, for $\hat{\varrho} = \sum_i p_i\hat{\varrho}_i$, i.e., a statistical mixture of density matrices, we have

$$F_q\left[\sum_i p_i\hat{\varrho}_i\right] \leqslant \sum_i p_i F_q[\hat{\varrho}_i]. \tag{16}$$

This property, applied to Eq. (12), gives

$$F_q \leqslant \iint d\vec{\alpha}\, d\vec{\beta}\, \mathcal{P}(\vec{\alpha},\vec{\beta})F_q^{(\vec{\alpha},\vec{\beta})}. \tag{17}$$

Here, $F_q^{(\vec{\alpha},\vec{\beta})}$ is the QFI calculated with a pure state $|\vec{\alpha},\vec{\beta};N\rangle$, thus it is given by Eq. (14).

We calculate the QFI for $\hat{J}_{\vec{n}} = \hat{J}_z$ and show that, for separable states, $F_q \leqslant N$. Any other direction $\vec{n}'$ can be obtained by a series of rotations of $\hat{J}_z$, generated by the operators (7). They are single-particle objects, therefore, once applied to the separable state (12) rather than to the evolution operator, they would transform one $\hat{\varrho}_{\rm sep}$ into another, i.e., would only change $\mathcal{P}(\vec{\alpha},\vec{\beta})$ into some $\tilde{\mathcal{P}}(\vec{\alpha},\vec{\beta})$ but will not modify the structure of Eq. (12). Thus it is enough to show that $F_q \leqslant N$ for $\hat{J}_z$ and a general probability distribution.

First, we calculate $F_q^{(\vec{\alpha},\vec{\beta})}$ with Eq. (14). The mean of $\hat{J}_z$ is

$$\langle \hat{J}_z\rangle = \frac{N}{2}\sum_n(|\alpha_n|^2 - |\beta_n|^2) \equiv \frac{N}{2}(|\vec{\alpha}|^2 - |\vec{\beta}|^2), \tag{18}$$

where we used the expression (6c) and the relation,

$$\hat{a}_n|\vec{\alpha},\vec{\beta};N\rangle = \sqrt{N}\alpha_n|\vec{\alpha},\vec{\beta};N-1\rangle, \tag{19a}$$

$$\hat{b}_n|\vec{\alpha},\vec{\beta};N\rangle = \sqrt{N}\beta_n|\vec{\alpha},\vec{\beta};N-1\rangle. \tag{19b}$$

The second moment is calculated in a similar way, i.e.,

$$\langle \hat{J}_z^2\rangle = \sum_{n,m}\langle \hat{J}_z^{(n)}\hat{J}_z^{(m)}\rangle = \sum_n \langle (\hat{J}_z^{(n)})^2\rangle + \sum_{n\neq m}\langle \hat{J}_z^{(n)}\hat{J}_z^{(m)}\rangle. \tag{20}$$

The two contributions must be treated separately,

$$\sum_n \langle (\hat{J}_z^{(n)})^2\rangle = \frac{N}{4}\left[1+(N-1)\sum_n(|\alpha_n|^2-|\beta_n|^2)^2\right],$$

$$\sum_{n\neq m}\langle \hat{J}_z^{(n)}\hat{J}_z^{(m)}\rangle = \frac{N(N-1)}{4} \times \sum_{n\neq m}(|\alpha_n|^2-|\beta_n|^2)(|\alpha_m|^2-|\beta_m|^2).$$

We add these two terms and obtain

$$\langle \hat{J}_z^2\rangle = \frac{N}{4}+\frac{N(N-1)}{4}(|\vec{\alpha}|^2-|\vec{\beta}|^2)^2. \tag{21}$$

The subtraction of the squared mean from Eq. (18) gives

$$0 \leqslant F_q^{(\vec{\alpha},\vec{\beta})} = N[1-(|\vec{\alpha}|^2-|\vec{\beta}|^2)^2] \leqslant N. \tag{22}$$

This result, combined with Eq. (17) yields

$$F_q \leqslant N. \tag{23}$$

Therefore, the QFI is limited by $N$ for the separable states of $N$ particles. However, the QFI can surpass this value, for instance, when the interferometer is fed with a particle-entangled two-region NOON state,

$$|\psi\rangle = \frac{1}{\sqrt{2}}(|N,0\rangle + |0,N\rangle). \tag{24}$$

Here $|N,0\rangle$ represents a configuration where all $N$ particles reside in one region only. For this state we have the Heisenberg scaling,

$$F_q = N^2. \tag{25}$$

Therefore, we conclude that the particle entanglement is the resource for the SSN metrology also in multimode systems. We now extend the above formalism to distinguishable particles.

### B. Distinguishable particles

#### 1. Multimode interferometric transformations

Note that the formalism of the second quantization allows for a quick generalization of the above results to distinguishable particles. Namely, another index must be attributed to the operators $\hat{a}_n$ and $\hat{b}_n$ such that labels the species of the particle (and of the associated field). This way, for the particle of type $j$, we obtain $\hat{a}_n^{(j)}$ and $\hat{b}_n^{(j)}$. The interferometric transformations cannot transmute a particle of one type into another—such a process would violate the conservation laws and the related superselection rules [45,48,49]. Thus a particle of each type undergoes a separate transformation, which means that the operators (6) change into

$$\hat{J}_x = \frac{1}{2}\sum_{j=1}^{N}\sum_n\left(\hat{a}_n^{(j)\dagger}\hat{b}_n^{(j)}+\hat{b}_n^{(j)\dagger}\hat{a}_n^{(j)}\right), \tag{26a}$$

$$\hat{J}_y = \frac{1}{2i}\sum_{j=1}^{N}\sum_n\left(\hat{a}_n^{(j)\dagger}\hat{b}_n^{(j)}-\hat{b}_n^{(j)\dagger}\hat{a}_n^{(j)}\right), \tag{26b}$$

$$\hat{J}_z = \frac{1}{2}\sum_{j=1}^{N}\sum_n\left(\hat{a}_n^{(j)\dagger}\hat{a}_n^{(j)}-\hat{b}_n^{(j)\dagger}\hat{b}_n^{(j)}\right). \tag{26c}$$

Once the interferometric transformations are determined, we discuss the role of the particle entanglement for the SSN sensitivity.

#### 2. Role of the particle entanglement

The separable state of $N$ distinguishable particles is constructed from the one-body pure states. For the particle of type $j$ distributed among $a$ and $b$ it reads

$$|\vec{\alpha}^{(j)},\vec{\beta}^{(j)};N\rangle = (\vec{\alpha}^{(j)}\hat{\vec{a}}^{(j)\dagger}+\vec{\beta}^{(j)}\hat{\vec{b}}^{(j)\dagger})|0\rangle. \tag{27}$$

The parallel with the coherent state from Eq. (11) is evident, and it is even more pronounced when the separable state of distinguishable particles is introduced

$$\hat{\varrho}_{\rm sep} = \iint d\vec{\alpha}^{(1)}d\vec{\beta}^{(1)}\cdots\iint d\vec{\alpha}^{(N)}d\vec{\beta}^{(N)} \times \mathcal{P}(\vec{\alpha}^{(1)},\vec{\beta}^{(1)},\ldots,\vec{\alpha}^{(N)},\vec{\beta}^{(N)}) \times \bigotimes_{i=1}^{N}|\vec{\alpha}^{(j)},\vec{\beta}^{(j)};N\rangle\langle\vec{\alpha}^{(j)},\vec{\beta}^{(j)};N|. \tag{28}$$

The state of $N$ distinguishable and nonentangled particles is the state (12) but with each mode—now labeled with two numbers $n$ and $j$ rather than with $n$ only—occupied with one particle. The deep analogy holds since the transformation (26) cannot transmute the particles.

Once this close relation is noticed, the QFI can be bounded from above in a similar fashion to that presented in Sec. II A 2 and the calculation is straightforward. We again pick the interferometric transformation to be generated by $\hat{J}_z$, and using the convexity of the QFI declared in Eq. (17), we have

$$F_q \leqslant \iint d\vec{\alpha}^{(1)}d\vec{\beta}^{(1)}\cdots\iint d\vec{\alpha}^{(N)}d\vec{\beta}^{(N)} \times \mathcal{P}(\vec{\alpha}^{(1)},\vec{\beta}^{(1)},\ldots,\vec{\alpha}^{(N)},\vec{\beta}^{(N)})\sum_{j=1}^{N}F_q^{(\vec{\alpha}^{(j)},\vec{\beta}^{(j)})}. \tag{29}$$

Here we used the fact that the operator (26c) acts on each particle independently. Every $F_q^{(\vec{\alpha}^{(j)},\vec{\beta}^{(j)})}$ is calculated with a single-particle state (27), therefore it is bounded as in Eq. (22) but with $N=1$ (because there is only a single particle of a given type), namely,

$$0 \leqslant F_q^{(\vec{\alpha}^{(j)},\vec{\beta}^{(j)})} = [1-(|\vec{\alpha}^{(j)}|^2-|\vec{\beta}^{(j)}|^2)^2] \leqslant 1. \tag{30}$$

Therefore the sum from Eq. (29) is bounded as follows:

$$\sum_{j=1}^{N} F_q^{(\vec{\alpha}^{(j)},\vec{\beta}^{(j)})} \leqslant N. \tag{31}$$

Since $\mathcal{P}$ from Eq. (29) is normalized we obtain

$$F_q \leqslant N \tag{32}$$

for all separable states of distinguishable particles defined in Eq. (28). On the other hand, take an entangled NOON state of $N$ distinguishable particles—for instance, each in the same spatial mode—in the form

$$|\psi\rangle = \frac{1}{\sqrt{2}}\left(\prod_{j=1}^{N}\hat{a}^{(j)\dagger} + \prod_{j=1}^{N}\hat{b}^{(j)\dagger}\right)|0\rangle. \tag{33}$$

This state will give $F_q = N^2$ (the Heisenberg scaling), therefore the QFI is a witness of particle entanglement also for distinguishable particles.

### C. Other cases

For the story to be complete we must consider two other possible cases. One is when the system contains both distinguishable particles and bosons, all together forming a separable state. Again, we repeat that the interferometric transformations—to be consistent with the conservation laws and the superselection rules—cannot transmute the particles from these two groups into each other. Therefore, since they form a separable state where the mode occupied by each particle can be addressed individually, the set of distinguishable particles and bosons can be treated separately. Thus to each of these sets the arguments from the above sections apply, so also in such a configuration the particle entanglement will be a necessary resource to beat the shot-noise limit.

Another possibility is that the system does not contain a fixed number of particles but rather its amount fluctuates from shot to shot governed by the probability distribution $P(N)$. The separable state is now

$$\hat{\varrho}_{\text{sep}} = \sum_{N=0}^{\infty} P(N)\hat{\varrho}_{\text{sep}}^{(N)}, \tag{34}$$

where $\hat{\varrho}_{\text{sep}}^{(N)}$ contains $N$ particles and is given either by Eq. (12) or (28) or by a mixture of those as discussed in the above paragraph. Since the operators $\hat{J}_i$ do not couple states with different numbers of particles, each fixed-$N$ sector can be treated separately. Therefore, using again the convexity of the QFI, in all the cases we obtain for separable states,

$$F_q \leqslant \sum_{N=0}^{\infty} P(N)N \equiv \langle N\rangle, \tag{35}$$

which defines the shot-noise limit [50].

Finally, we note that these arguments do not apply to collections of fermions for which the separable states do not exist due to the Pauli exclusion principle.

## III. ESTIMATION FROM THE MEAN POPULATION IMBALANCE

We now abandon the general considerations and switch to a particular phase estimation protocol. We derive the phase sensitivity for a multimode Mach-Zehnder interferometer (MZI). We take the most common estimation protocol where the phase is deduced from the average population imbalance between the two regions. Although the derivation is performed for bosons, according to the above arguments the results apply also to distinguishable particles and collections of both.

In analogy to the two-mode case, the multimode MZI evolution operator is

$$\hat{U}(\theta) = e^{-i\theta\hat{J}_y}, \tag{36}$$

with the generator given by Eq. (7b). At the output, in the $i$th repetition of the experiment, the number of particles in each arm is measured, i.e., $n_a^{(i)}$ and $n_b^{(i)}$. From these data, the population imbalance between the two subsystems is calculated $n_i = \frac{n_a^{(i)} - n_b^{(i)}}{2}$, and the sequence is repeated $m$ times and averaged to give

$$\overline{n}_m = \frac{1}{m}\sum_{i=1}^{m} n_i. \tag{37}$$

If $m \gg 1$, the central limit theorem tells that the probability for obtaining $\overline{n}_m$ is a Gaussian function,

$$p(\overline{n}_m) \propto \exp\left[-m\frac{[\overline{n}_m - \langle\hat{J}_z(\theta)\rangle]^2}{2\langle[\Delta\hat{J}_z(\theta)]^2\rangle}\right]. \tag{38}$$

When the phase is estimated from the maximum of the likelihood function for this probability, we obtain the variance of the estimator, i.e., the sensitivity,

$$\Delta^2\theta = \frac{1}{m}\frac{\langle[\Delta\hat{J}_z(\theta)]^2\rangle}{\left(\frac{\partial\langle\hat{J}_z(\theta)\rangle}{\partial\theta}\right)^2}. \tag{39}$$

$\hat{J}_z(\theta)$ is obtained by evolving $\hat{J}_z$ with the operator (36), i.e.,

$$\hat{J}_z(\theta) = \hat{U}^\dagger(\theta)\hat{J}_z\hat{U}(\theta) = \hat{J}_z\cos\theta + \hat{J}_x\sin\theta, \tag{40}$$

where the last equality was obtained using the commutation relations of operators (6) and the Baker-Campbell-Hausdorff formula. Substitution of the result (40) into Eq. (39) gives for $\theta = 0$,

$$\Delta^2\theta = \frac{1}{m}\frac{\langle(\Delta\hat{J}_z)^2\rangle}{\langle\hat{J}_x\rangle^2}. \tag{41}$$

This is a natural extension of the spin-squeezing parameter (for balanced systems, where $\langle\hat{J}_y\rangle = 0$) to the multimode case. The combination of Eqs. (13) and (23) means that also the following ratio:

$$\xi^2 \equiv N\frac{\langle(\Delta\hat{J}_z)^2\rangle}{\langle\hat{J}_x\rangle^2} \tag{42}$$

is a witness of quantum correlations among the particles—when $\xi^2 < 1$ the system is particle entangled. We now show that the measurement of this quantity in the multimode system is not as straightforward as in the two-mode case.

## IV. DETECTION OF ENTANGLEMENT—FLUCTUATIONS AND VISIBILITY

First however we recall that, for the two-mode systems, the spin-squeezing parameter is defined as

$$\xi_S^2 = N\frac{\langle(\Delta\hat{J}_3)^2\rangle}{\langle\hat{J}_1\rangle^2+\langle\hat{J}_2\rangle^2}. \tag{43}$$

Here 1, 2, and 3 are three orthogonal directions obtained by the combinations of $\hat{J}_x$, $\hat{J}_y$, and $\hat{J}_z$ from Eqs. (6). When $\xi_S^2<1$, the system is spin squeezed—it is particle entangled and useful for quantum metrology [22]. It it most common to take (1,2,3) as $(x,y,z)$, giving

$$\xi_S^2 = N\frac{\langle(\Delta\hat{J}_z)^2\rangle}{\langle\hat{J}_x\rangle^2+\langle\hat{J}_y\rangle^2}. \tag{44}$$

The motivation for this particular choice lies in direct experimental accessibility both to the nominator and to the denominator of Eq. (44). This can be seen particularly easily when the average number of atoms in each mode is high. In this case, the mode operators can be approximated as follows:

$$\hat{a}\simeq\sqrt{n_a}e^{i(\phi/2)},\quad \hat{b}\simeq\sqrt{n_b}e^{-i(\phi/2)}. \tag{45}$$

Here, $n_{a/b}$ are the average mode occupations, and $\phi$ is the relative phase, which fluctuates from shot to shot. In this approximation, the average of $\hat{J}_x$ and $\hat{J}_y$ is

$$\langle\hat{J}_x\rangle=\sqrt{n_an_b}\langle\cos\phi\rangle,\quad \langle\hat{J}_y\rangle=\sqrt{n_an_b}\langle\sin\phi\rangle. \tag{46}$$

Similarly, the atom number fluctuations normalized to the shot noise is

$$\xi_N^2 = N\frac{\langle(\Delta\hat{J}_z)^2\rangle}{n_an_b}. \tag{47}$$

Therefore, the spin squeezing from Eq. (44) can be expressed as follows:

$$\xi_S^2=\frac{\xi_N^2}{\langle\cos\phi\rangle^2+\langle\sin\phi\rangle^2}. \tag{48}$$

Note that, for the spin-coherent state $\xi_N^2\equiv1$, although the phase is fixed and does not fluctuate from shot to shot so that $\langle\cos\phi\rangle^2+\langle\sin\phi\rangle^2=\cos^2\phi+\sin^2\phi=1$, giving $\xi_S^2=1$, the system is not spin squeezed. In the experiments, the atom number fluctuations are calculated by measuring in each shot the population of each mode. In another series of experiments, the two modes are let to interfere, and the relative phase of the pattern is recorded to give, after many runs, the denominator of Eq. (48).

Note that there is an alternative method for measuring (44), which does not rely on the mean-field approximation (45). In the far field, the spatial wave packet of modes $a$ and $b$ are plane waves (or, more precisely, broad functions with fast oscillations on top), i.e.,

$$\hat{\Psi}(x)=e^{ikx}\hat{a}+e^{-ikx}\hat{b}. \tag{49}$$

The density of this system is

$$\rho(x)=\langle\hat{\Psi}^\dagger(x)\hat{\Psi}(x)\rangle=\langle\hat{a}^\dagger\hat{a}\rangle+\langle\hat{b}^\dagger\hat{b}\rangle+2\langle\hat{J}_x\rangle\cos(2kx)+2\langle\hat{J}_y\rangle\sin(2kx). \tag{50}$$

Since $\langle\hat{a}^\dagger\hat{a}\rangle+\langle\hat{b}^\dagger\hat{b}\rangle=N$, the normalized density reads

$$p(x)=\frac{1}{N}\rho(x)=1+\nu_1\cos(2kx)+\nu_2\sin(2kx)=1+\nu\cos(2kx-\alpha), \tag{51}$$

where $\nu_{1/2}=\frac{2}{N}\langle\hat{J}_{x/y}\rangle$ and $\alpha=\arccos(\frac{\nu_1}{\nu})$, whereas $\nu=\sqrt{\nu_1^2+\nu_2^2}$ is the fringe visibility. Therefore, the spin-squeezing (44) can be expressed in terms of the atom number fluctuations $\eta^2=\frac{4}{N}\langle(\Delta\hat{J}_z)^2\rangle$ and the visibility,

$$\xi_S^2=\frac{\eta^2}{\nu^2}. \tag{52}$$

We now demonstrate that the use of this operational definition of the spin squeezing without the *a priori* knowledge about the mode structure of each arm can lead to false conclusions regarding the presence of the particle entanglement in the system.

In the multimode case, the density calculated with the operator (2) is

$$\rho(x)=\rho_{aa}(x)+\rho_{bb}(x)+\rho_{ab}(x)+\rho_{ba}(x), \tag{53}$$

where $\rho_{ij}(x)=\langle\hat{\Psi}_i^\dagger(x)\hat{\Psi}_j^\dagger(x)\rangle$. Clearly the density contains multiple interference terms not only resulting from the overlap of the wave functions coming from the opposite regions, but also from different modes residing initially in the same region. Therefore, the visibility of fringes cannot be linked to the denominator of Eq. (42), which only quantifies the $a/b$ coherence. For illustration, take a coherent spin state from Eq. (9) with $\varphi=0$. Assume now that, in region $a$, some process splits mode $a$ into the coherent superposition of $a_1$ and $a_2$, schematically shown in Fig. 2 in a double-well setup.

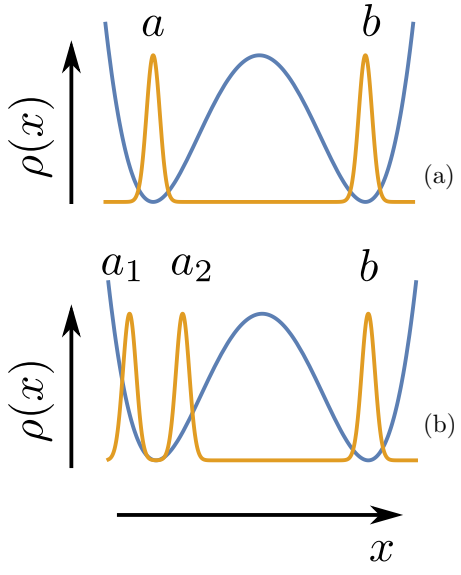


FIG. 2. The single-particle density of atoms trapped in a double-well potential. (a) The standard two-mode setup. (b) The three-mode setup: the configuration after a coherent splitting of the $a$ mode into $a_1$ and $a_2$.

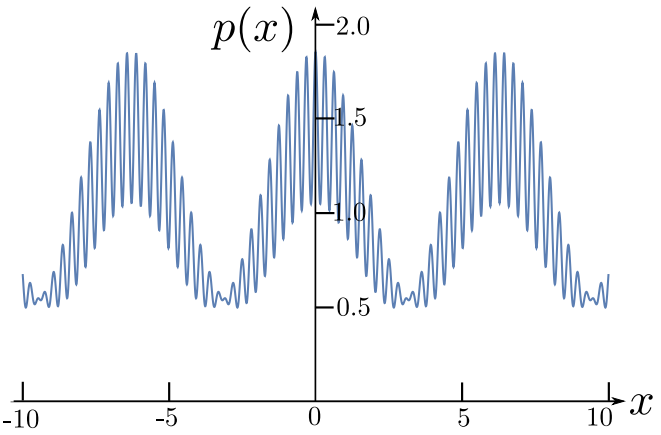


FIG. 3. The single-particle far-field interference pattern, see Eq. (56), formed by a coherent spin-state (54) in the three-mode configuration shown in Fig. 2(b). The parameters are $z = 0.91$, $\zeta = 0.5$, $k = 10$, and $\delta k = 0.5$.

This way, a state,

$$|\psi\rangle = \frac{1}{\sqrt{N!}}[\sqrt{z}(\sqrt{\zeta}\hat{a}_1^\dagger + \sqrt{1-\zeta}\hat{a}_2^\dagger) + \sqrt{1-z}\hat{b}_1^\dagger]^N|0\rangle \quad (54)$$

is obtained. It is an example of a nonentangled state from Eq. (11) with $\vec{\alpha} = \sqrt{z}(\sqrt{\zeta},\sqrt{1-\zeta},0\cdots)^T$ and $\vec{\beta} = (\sqrt{1-z},0\cdots)^T$. The splitting does not influence the nominator of Eq. (42), but in the far field the interference of the two modes $a_1$ and $a_2$ will have an impact on the visibility of fringes. The field operator after the expansion will read

$$\hat{\Psi}(x) = e^{i(k+\delta k)x}\hat{a}_1 + e^{i(k-\delta k)x}\hat{a}_2 + e^{-ikx}\hat{b}, \quad (55)$$

giving the normalized density,

$$\begin{aligned} p(x) &= \frac{1}{N}\langle\hat{\Psi}^\dagger(x)\hat{\Psi}(x)\rangle \\ &= 1 + z\sqrt{\zeta(1-\zeta)}\cos(2\delta k x) \\ &\quad + \sqrt{z(1-z)}\{\sqrt{\zeta}\cos[(2k+\delta k)x] \\ &\quad + \sqrt{1-\zeta}\cos[(2k-\delta k)x]\}. \end{aligned} \quad (56)$$

This density is plotted in Fig. 3 with $z = 0.91$, $\zeta = 0.5$, $k = 10$, and $\delta k = 0.5$ (in dimensionless units). The fringe visibility, calculated as the ratio $\nu = (p_{\max} - p_{\min})/(p_{\max} + p_{\min})$ is $\nu^2 = 0.326$. This combined with the normalized population imbalance between the two regions $\eta^2 = 1 - (2z-1)^2 = 0.321$ gives the ratio $\eta^2/\nu^2 = 0.988$, suggesting the presence of the particle entanglement in the system. However, it is a false statement: $\nu$ cannot be identified with the denominator of Eq. (42) in this case.

*Some remarks*. Naturally, the three-mode example invoked here is quite artificial. It is hard to imagine that a coherent physical process, which splits $\hat{a}$ into $\hat{a}_1$ and $\hat{a}_2$ could be uncontrolled and unnoticed by the experimentalists. Also, any experimentalist would immediately notice two frequencies of oscillations in the interference pattern. Last but not least, usually the multimode structure of the two regions $a$ and $b$ comes from the thermal excitations and thus reveals no coherence between the modes. Nevertheless, the example shows that the method of detecting the particle entanglement through the fluctuations-to-visibility ratio can be used safely only when the structure of each subsystem is known.

## V. SUMMARY

The main outcome of this paper is the establishment of the SNL for the two-arm multimode interferometers. This is a general result as it applies to any thinkable quantum system where the entangled or nonentangled dichotomy exists. It is valid for both fixed- and non-fixed-$N$ systems for as long as the coherence between states carrying a different number of particles is absent. It turns out that the additional modes do not improve the sensitivity for as long as they are not interacting. Therefore, if $\Delta\theta$ beats the shot-noise level established for the two-mode systems, this also signals the presence of the useful particle entanglement in the complex multimode case.

Note that our results are valid for a particular choice of the interferometric transformations such that do not penetrate the inner structure of each arm but rather treat them as a whole. In principle, any other type of such a transformation requires a dedicated calculation of the SNL. Otherwise, conclusions about the presence of metrologically useful particle entanglement in the system can be incorrect.

We also have calculated the phase sensitivity for the standard estimation protocol based on the knowledge of the mean population imbalance between the two arms. Finally, we have shown that, if the popular method of detecting the entanglement in two-mode systems is used without the *a priori* knowledge about the modal structure of the arms, a false conclusion from the number-fluctuations-to-visibility ratio can drawn.

[1] R. A. Schumacher, Am. J. Phys. **62**, 609 (1994).
[2] B. P. Abbott *et al.*, Phys. Rev. Lett. **116**, 061102 (2016).
[3] K. S. Hardman, P. J. Everitt, G. D. McDonald, P. Manju, P. B. Wigley, M. A. Sooriyabandara, C. C. N. Kuhn, J. E. Debs, J. D. Close, and N. P. Robins, Phys. Rev. Lett. **117**, 138501 (2016).
[4] G. Ferrari, N. Poli, F. Sorrentino, and G. M. Tino, Phys. Rev. Lett. **97**, 060402 (2006).
[5] N. Poli, F.-Y. Wang, M. G. Tarallo, A. Alberti, M. Prevedelli, and G. M. Tino, Phys. Rev. Lett. **106**, 038501 (2011).
[6] M. J. Snadden, J. M. McGuirk, P. Bouyer, K. G. Haritos, and M. A. Kasevich, Phys. Rev. Lett. **81**, 971 (1998).
[7] J. M. McGuirk, M. J. Snadden, and M. A. Kasevich, Phys. Rev. Lett. **85**, 4498 (2000).
[8] J. M. McGuirk, G. T. Foster, J. B. Fixler, M. J. Snadden, and M. A. Kasevich, Phys. Rev. A **65**, 033608 (2002).
[9] M. Andia, R. Jannin, F. Nez, F. Biraben, S. Guellati-Khélifa, and P. Cladé, Phys. Rev. A **88**, 031605(R) (2013).
[10] M. Antezza, L. P. Pitaevskii, and S. Stringari, Phys. Rev. A **70**, 053619 (2004).

[11] I. Carusotto, L. Pitaevskii, S. Stringari, G. Modugno, and M. Inguscio, Phys. Rev. Lett. **95**, 093202 (2005).
[12] D. M. Harber, J. M. Obrecht, J. M. McGuirk, and E. A. Cornell, Phys. Rev. A **72**, 033610 (2005).
[13] J. M. Obrecht, R. J. Wild, M. Antezza, L. P. Pitaevskii, S. Stringari, and E. A. Cornell, Phys. Rev. Lett. **98**, 063201 (2007).
[14] J. Chwedeńczuk, L. Pezzé, F. Piazza, and A. Smerzi, Phys. Rev. A **82**, 032104 (2010).
[15] G. Lamporesi, A. Bertoldi, L. Cacciapuoti, M. Prevedelli, and G. M. Tino, Phys. Rev. Lett. **100**, 050801 (2008).
[16] G. Rosi, L. Cacciapuoti, F. Sorrentino, M. Menchetti, M. Prevedelli, and G. M. Tino, Phys. Rev. Lett. **114**, 013001 (2015).
[17] P. Cladé, E. de Mirandes, M. Cadoret, S. Guellati-Khélifa, C. Schwob, F. Nez, L. Julien, and F. Biraben, Phys. Rev. A **74**, 052109 (2006).
[18] R. Bouchendira, P. Cladé, S. Guellati-Khélifa, F. Nez, and F. Biraben, Phys. Rev. Lett. **106**, 080801 (2011).
[19] P. Cladé, E. de Mirandes, M. Cadoret, S. Guellati-Khélifa, C. Schwob, F. Nez, L. Julien, and F. Biraben, Phys. Rev. Lett. **96**, 033001 (2006).
[20] R. Battesti, P. Cladé, S. Guellati-Khélifa, C. Schwob, B. Grémaud, F. Nez, L. Julien, and F. Biraben, Phys. Rev. Lett. **92**, 253001 (2004).
[21] M. Cadoret, E. de Mirandes, P. Cladé, S. Guellati-Khélifa, C. Schwob, F. Nez, L. Julien, and F. Biraben, Phys. Rev. Lett. **101**, 230801 (2008).
[22] V. Giovannetti, S. Lloyd, and L. Maccone, Science **306**, 1330 (2004).
[23] L. Pezzé and A. Smerzi, Phys. Rev. Lett. **102**, 100401 (2009).
[24] LIGO Scientific Collaboration, Nat. Phys. **7**, 962 (2011).
[25] J. Esteve, C. Gross, A. Weller, S. Giovanazzi, and M. Oberthaler, Nature (London) **455**, 1216 (2008).
[26] T. Berrada, S. van Frank, R. Bücker, T. Schumm, J.-F. Schaff, and J. Schmiedmayer, Nat. Commun. **4**, 2077 (2013).
[27] I. D. Leroux, M. H. Schleier-Smith, and V. Vuletić, Phys. Rev. Lett. **104**, 250801 (2010).
[28] Z. Chen, J. G. Bohnet, S. R. Sankar, J. Dai, and J. K. Thompson, Phys. Rev. Lett. **106**, 133601 (2011).
[29] C. Gross, T. Zibold, E. Nicklas, J. Esteve, and M. K. Oberthaler, Nature (London) **464**, 1165 (2010).
[30] J. Appel, P. J. Windpassinger, D. Oblak, U. B. Hoff, N. Kjærgaard, and E. S. Polzik, Proc. Natl. Acad. Sci. USA **106**, 10960 (2009).
[31] M. Kitagawa and M. Ueda, Phys. Rev. A **47**, 5138 (1993).
[32] D. J. Wineland, J. J. Bollinger, W. M. Itano, and D. J. Heinzen, Phys. Rev. A **50**, 67 (1994).
[33] B. Lücke, M. Scherer, J. Kruse, L. Pezzé, F. Deuretzbacher, P. Hyllus, J. Peise, W. Ertmer, J. Arlt, L. Santos *et al.*, Science **334**, 773 (2011).
[34] R. Bücker, J. Grond, S. Manz, T. Berrada, T. Betz, C. Koller, U. Hohenester, T. Schumm, A. Perrin, and J. Schmiedmayer, Nat. Phys. **7**, 608 (2011).
[35] K. V. Kheruntsyan, J.-C. Jaskula, P. Deuar, M. Bonneau, G. B. Partridge, J. Ruaudel, R. Lopes, D. Boiron, and C. I. Westbrook, Phys. Rev. Lett. **108**, 260401 (2012).
[36] A. Perrin, H. Chang, V. Krachmalnicoff, M. Schellekens, D. Boiron, A. Aspect, and C. I. Westbrook, Phys. Rev. Lett. **99**, 150405 (2007).
[37] W. RuGway, S. S. Hodgman, R. G. Dall, M. T. Johnsson, and A. G. Truscott, Phys. Rev. Lett. **107**, 075301 (2011).
[38] E. Andersson, T. Calarco, R. Folman, M. Andersson, B. Hessmo, and J. Schmiedmayer, Phys. Rev. Lett. **88**, 100401 (2002).
[39] T. Wasak, P. Szańkowski, R. Bücker, J. Chwedeńczuk, and M. Trippenbach, New J. Phys. **16**, 013041 (2014).
[40] Note that, in principle, an interferometer can be a series of linear transformations rather than a single one [14]. Still, such a composite operation remains linear and does not entangle the particles.
[41] R. J. Glauber, Phys. Rev. **131**, 2766 (1963).
[42] E. C. G. Sudarshan, Phys. Rev. Lett. **10**, 277 (1963).
[43] T. Wasak, P. Szańkowski, P. Ziń, M. Trippenbach, and J. Chwedeńczuk, Phys. Rev. A **90**, 033616 (2014).
[44] T. Wasak, P. Szańkowski, M. Trippenbach, and J. Chwedeńczuk, Quantum Inf. Process. **15**, 269 (2015).
[45] T. Wasak, A. Smerzi, and J. Chwedeńczuk, arXiv:1609.01576.
[46] A. S. Holevo, *Probabilistic and Statistical Aspects of Quantum Theory* (Scuola Normale Superiore Pisa, Pisa, Italy, 2011).
[47] S. L. Braunstein and C. M. Caves, Phys. Rev. Lett. **72**, 3439 (1994).
[48] G. C. Wick, A. S. Wightman, and E. P. Wigner, Phys. Rev. **88**, 101 (1952).
[49] S. D. Bartlett, T. Rudolph, and R. W. Spekkens, Rev. Mod. Phys. **79**, 555 (2007).
[50] P. Hyllus, L. Pezzé, and A. Smerzi, Phys. Rev. Lett. **105**, 120501 (2010).